American Mineralogist, Volume 85, pages 189–193, 2000

The nuclear and magnetic structure of "white rust"—$Fe(OH_{0.86}D_{0.14})_2$

**JOHN B. PARISE,[1,*] WILLIAM G. MARSHALL,[2] RONALD I. SMITH,[2] H.D. LUTZ,[3]
AND HENDRIK MÖLLER[3]**

[1]CENTER FOR HIGH PRESSURE RESEARCH AND DEPARTMENT OF GEOSCIENCES AND DEPARTMENT OF CHEMISTRY, STATE UNIVERSITY OF NEW YORK,
STONY BROOK, NEW YORK 11794-3400, U.S.A.
[2]ISIS Neutron Facility, CLRC Rutherford Appleton Laboratory, Chilton, Didcot, Oxon OX11 0QX, U.K.
[3]Anorganische Chemie I, Universität Siegen, D-57068 Siegen, Germany

ABSTRACT

The structure of $Fe(OH_{0.86},OD_{0.14})_2$ was refined by applying the Rietveld technique to neutron powder diffraction data collected at 300, 150, and 10 K. The nuclear structure, of the CdI_2 type ($P\bar{3}m1$) and isostructural with Mg, Ca, Mn, Ni, and β-$Co(OH)_2$, is maintained over the range of temperatures studied. At 10 K, the magnetic structure is ordered antiferromagnetically, with the magnetic moments aligned in the basal plane. The refined Fe^{2+} magnetic moment magnitude is 3.50(4) μ_B. This magnetic structure (space group $P_{2c}\bar{1}$) is unique amongst those encountered in the transition metal dihydroxides, for which the moment is either directed along the *c* axis [β-$Co(OH)_2$ and $Ni(OH)_2$], or at least has a considerable component along this direction [$Mn(OH)_2$]. The dependence of the strength of potential hydrogen bonds with temperature is discussed.

INTRODUCTION

Several studies of the nuclear and magnetic structures of layered transition element hydroxides possessing the CdI_2 structure have been reported (Christensen and Ollivier 1972; Greaves and Thomas 1986; Parise et al. 1998a, 1994; Szytula et al. 1971) but studies of $Fe(OH)_2$ are rare (Lutz et al. 1994a). This is not unexpected because this material's sensitivity to oxidation and pyrophoric behavior in the atmosphere make pure samples of "white rust" difficult to obtain. A better understanding of its structures and magnetism, however, are desirable given the importance of $Fe(OH)_2$ in the early stages of corrosion (Castro and Vilche 1991) and its possible role in microbial action in the environment (Ivanov et al. 1997), which were studied using magnetic techniques (Verkhovtseva et al. 1991).

The CdI_2-related hydroxides in general are obvious model systems for the investigation of hydrogen bonding in solids (Fig. 1). This unique structure has hydrogen atoms isolated between layers of metal ions in octahedral coordination with oxygen. This arrangement allows both O-H···O and H···H interactions to be studied in a series of isostructural materials with variable metal acidity (Sherman 1991) and *c*/*a*-ratio. Several theoretical (D'Arco et al. 1993; Sherman 1991), neutron diffraction (Catti et al. 1995; Desgranges et al. 1996, 1993; Lutz et al. 1994a; Parise et al. 1998a, 1998b) and spectroscopic (Beckenkamp and Lutz 1992; Duffy et al. 1995; Kruger et al. 1989; Lutz 1995; Lutz et al. 1994a, 1994b, 1995; Lutz and Jung 1997; Nguyen et al. 1994, 1997) investigations concentrated on characterizing the structures of these materials at both ambient and high pressure with the aim of understanding the details of hydrogen bonding. Although the pressure variable is ideal for the study of these interactions, because large changes in the *c* axis are expected in these highly anisotropic materials, low temperature can provide a complementary variable to study the details of these interactions (Hazen and Finger 1982).

Earlier low temperature investigations of the magnetic interactions in these layered systems (Christensen and Ollivier 1972; Szytula et al. 1971) suggest differences in the magnetic ordering at low temperatures, with the moment antiferromagnetically ordered along the *c* axis in the case of $Ni(OH)_2$ (Szytula et al. 1971) and canted off the *c* axis in the case for $Mn(OH)_2$ (Christensen and Ollivier 1972). Preliminary results (Parise and Marshall in preparation) suggest that the magnetic structure of β-$Co(OH)_2$ is similar to that of $Ni(OD)_2$, and earlier measurements of the temperature dependence of the magnetic susceptibility show characteristic maxima for antiferromagnetic behavior at temperatures of 34 K for $Fe(OH)_2$, 30 K for $Ni(OH)_2$, and 12.3 K for $Co(OH)_2$. Although the magnetic structures of the Ni, Mn, and Co hydroxides have been investigated (Christensen and Ollivier 1972; Greaves and Thomas 1986; Szytula et al. 1971), and are considered established, that of $Fe(OH)_2$ remains unknown. This material was characterized by neutron diffraction at room temperature (Lutz et al. 1994a) but no description of its low temperature structure has been reported. We investigated the structure of this material above and below the magnetic ordering temperature, determined its magnetic structure and found it to be unique among the CdI_2-related hydroxides.

---

*E-mail: John.Parise@sunysb.edu

0003-004X/00/0001–0189$05.00

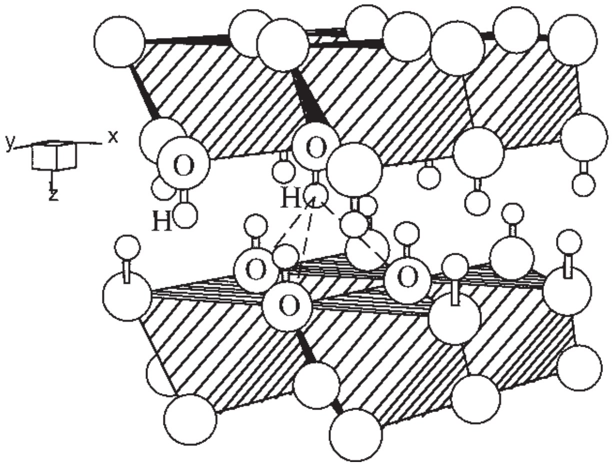

FIGURE 1. Structure of CdI_2-type (*Pm*1) hydroxides. The lines indicate tri-furcated H-bonds between H at ($^1/_3$,$^2/_3$, *z*) and O.

EXPERIMENTAL METHODS

The sample of $Fe(OH,OD)_2$ was prepared following previously published procedures (Lutz et al. 1994a). The sample was used for spectroscopic investigations of isotopically dilute systems and so contained both hydrogen and deuterium. Neutron powder diffraction data were collected in a closed cycle refrigeration unit at 300, 150, and 10 K on the POLARIS diffractometer at the UK pulsed spallation neutron source ISIS, Rutherford Appleton Laboratory. Data were collected in six banks of detectors centered at $2\theta = \pm35°$, ±90°, and ±145° for a total of 885, 826, and 501 μA.h at 10, 150, and 300 K, respectively. After focusing patterns from individual detectors, three histograms representative of the data collected at $2\theta = 35°$, 90°, and 145° were used in the subsequent Rietveld refinements.

Inspection of the data clearly shows the appearance of extra reflections in the data set collected at 10 K (Fig. 2). The appearance of prominent new peaks at *d*-spacings corresponding to the nuclear cell (0,0,$^1/_2$) and (0,0,$^3/_2$) reflections immediately excludes antiferromagnetic ordering with magnetic moments aligned along the *c* axis. Subsequent analysis of the 10 K diffraction data revealed a simple commensurate antiferromagnetic structure, consisting of a doubled nuclear cell along the *c* axis (Fig. 1), with the ordered Fe^{2+} magnetic moments lying in the basal plane (magnetic space group $P_{2c}\bar{1}$). Because no distortion of the nuclear cell accompanies the magnetic ordering, no distinction could be made concerning the moment orientation within the basal plane.

Structure refinement was performed using the Rietveld methodology (Rietveld 1969) as implemented in the General Structure Analysis System (GSAS) of programs (Larson and Von Dreele 1986). Starting values for the nuclear structure were taken from the literature (Lutz et al. 1994a) and the structures at 300 K and 150 K quickly converged to the models summarized in Table 1. Several models for the H-position in $Fe(OH_{0.86}OD_{0.14})_2$ were tried. Published structures for the CdI_2-related hydroxides often report on the disorder of this site (Desgranges et al. 1996, 1993; Megaw 1958; Parise et al. 1998b; Partin et al. 1994). This disorder is acute at high pressures, where avoidance of H...H repulsion (Parise et al. 1999) causes the proton to be displaced from the $\bar{3}$–axis. The disorder can be modeled with either an anisotropic displacement ellipsoid or as a partially occupied threefold site at (*x* , *x*, *z*, with $x < {}^1/_3$ or $x > {}^1/_3$). The anisotropic displacement model was adopted in this case, because both models provided the same agreement for the same number of parameters varied and the ratio U_{11}/U_{33} (Table 1) was less than two.

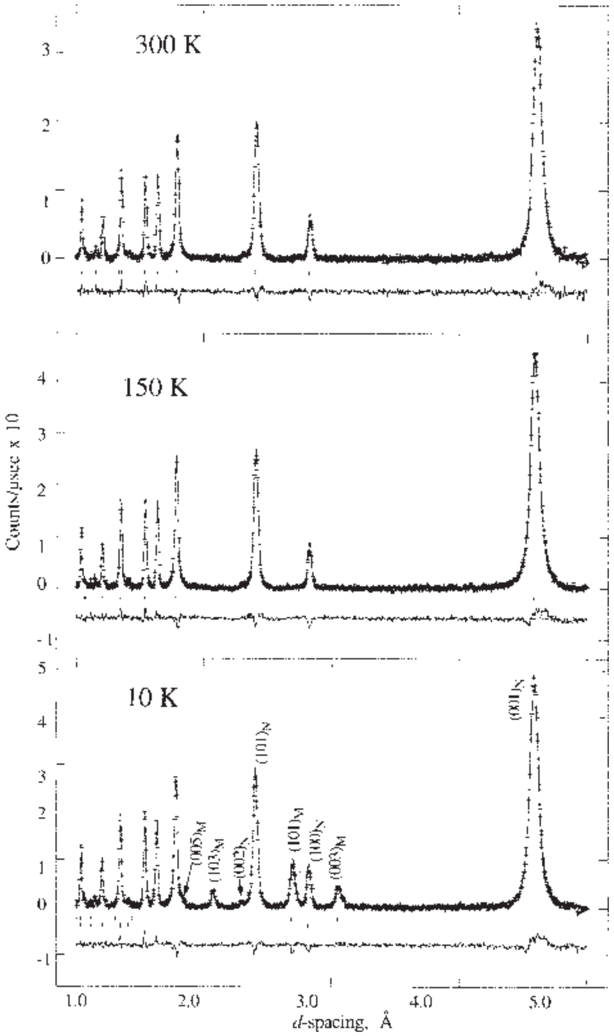

FIGURE 2. Rietveld fit to the data collected at 300, 150, and 10 K for the detectors in the 35° bank for $Fe(OH_{0.86}D_{0.14})_2$. Some of the nuclear (N) and magnetic (M) peaks are indicated for the data collected at 10 K. Crosses represent observed data, the continuous line is the profile calculated from the nuclear and magnetic structure model, and the line below is the difference between the two, plotted on the same scale.

The proportions of hydrogen and deuterium occupying the same crystallographic site were determined at each temperature by refinement of the site occupancy factor. The values obtained at each temperature are in good agreement (Table 1) with each other and with the previous spectroscopic study (0.85) of Lutz et al. (1994a). A single additional variable, the moment magnitude, was required to describe the magnetic structure, all remaining parameters (cell constants, phase fraction, reflection line shape)

TABLE 1. Selected refined parameters for $Fe(OH_{0.86}OD_{0.14})_2$*

	Temperature		
	10 K	150 K	300 K
a (Å)	3.25919(5)	3.26238(5)	3.26515(6)
c (Å)	4.5765(1)	4.5822(1)	4.6013(1)
z(O)	0.2234(1)	0.2226(1)	0.2213(2)
z(H)	0.4202(7)	0.4129(10)	0.4111(13)
Occupancy (H)	0.857(2)	0.863(2)	0.864(2)
μ_{Fe}/μ_B	3.50(4)	–	–
U_{iso}(Fe)†	0.22(1)	0.39(1)	0.73(2)
U_{iso}(O)†	0.32(1)	0.45(1)	0.68(2)
U_{11}(H)†	4.13(8)	4.37(8)	5.32(11)
U_{33}(H)†	2.8(2)	4.0(2)	3.9(3)
U_{12}(H)†	2.07(4)	2.18(4)	2.66(6)
U_{iso}(H)†	3.94(7)	4.31(8)	5.0(1)
χ^2 ‡	4.35	3.52	2.17
R_{wp},(%) ‡	1.7	1.6	1.6
$R_C(F^2)$ (%)§	3.34	2.99	4.32
$R_E(F^2)$ (%)§	4.87	3.29	6.40
$R_A(F^2)$ (%)§	8.83	4.67	9.33

* Space group $P\bar{3}m1$, Fe at (0, 0, 0), O at (⅓, ⅔, z ≈0.2), H/D sited on ideal position (2d) at (⅓, ⅔, z ≈ 0.4).

† Except for the U_{iso}(H) values, all the results shown are those obtained from the refinements in which H was refined anisotropically. All displacement parameter values are 100 × U (Å^2).

‡ Discrepancy index: $R_{wp} = \left[\sum_i w_i (y_i^o - \frac{1}{C} y_i^c)^2 / \sum_i w_i (y_i^o)^2\right]^{1/2}$ where y^o, y^c = observed and calculated profile intensities; C = scale factor; w_i = weight of individual profile intensity i.

§ Discrepancy index based on integrated Bragg intensities for individual banks of data at 145° (C), 90° (E), and 35° (A).

being constrained to the nuclear structure parameters.

RESULTS AND DISCUSSION

Description of the structure

Bond distances of $Fe(OH_{0.86}D_{0.14})_2$ at 10, 150, and 300 K are given in Table 2. Whereas the intralayer distances are practically independent of temperature, the interlayer O···O, H···H, and H···O distances are significantly shortened on going down to 10 K. This is reflected in the decrease in the *c/a* ratio of the lattice constants, e.g., 1.4092 at 300 K and 1.4042 at 10 K. Thus, the H···O distances, which are relevant for the presence or absence of hydrogen bonds, change from 2.533 Å at 300 K to 2.490 Å at 10 K. The change of the O–H interatomic distance from 0.87 Å to 0.90 Å between ambient temperature and 10 K is mainly caused by the decrease of the librational mode amplitudes. The apparent length itself is somewhat shorter and this is expected for models placing the hydrogen on the threefold axis (Parise et al. 1998a). The use of a split-site model, however, with H atoms distributed over the 6*i* sites rather than 3*d* in space group ($P\bar{3}m1$) or correction for thermal motion would increase the bond distance. Another possible source of systematic error is the complex anisotropic line-shape function (Larson and Von Dreele 1986) required to fit the diffraction profiles (Fig. 2). The synthetic conditions used (Lutz et al. 1994a) promote the precipitation of material with small particle size and stacking faults. This can be avoided in other hydroxides by post-synthesis hydrothermal treatment (Parise et al. 1994, 1998a) and would lead to decomposition and the introduction of impurities in the case of $Fe(OH,OD)_2$.

Hydrogen bonds

The potential existence of hydrogen bonds in brucite-type hydroxides has a somewhat controversial history and has been discussed in detail over the last ten years (Beckenkamp and Lutz 1992; Duffy et al. 1995; Kruger et al. 1989; Lutz 1995; Lutz et al. 1994a, 1994b, 1995, 1997; Nguyen et al. 1994, 1997; Parise et al. 1998a, 1998b, 1999). If the presence of weak trifurcated hydrogen bonds in brucite-type transition-metal hydroxides is true as claimed (Parise et al. 1994), the strength of these bonds is nearly equal for $Ni(OH)_2$, $Mn(OH)_2$, $Fe(OH)_2$, β-$Co(OH)_2$, and $Cd(OH)_2$ as shown by the nearly constant wavenumbers of the respective OH stretching modes; 3610, 3602, 3600, 3598, and 3587 cm^{-1} are the mean values of the IR and the Raman allowed bands at ambient temperature (Lutz et al. 1994a).

At liquid helium temperature, the strength of the potential hydrogen bonds should be changed. Thus, the wavenumber of the uncoupled OD stretching mode (isotopically dilute sample) of $Fe(OH_{0.86}D_{0.14})_2$ increases from 2656 cm^{-1} (295 K) to 2662 cm^{-1} (95 K) (Lutz et al. 1994a). A positive temperature shift of OH and OD stretching modes has been attributed to the presence of highly bent or bifurcated hydrogen bonds, as well as to hydroxide ions, which are not involved in hydrogen bonding (Lutz 1995). The interlayer H···O and O···O distances decrease from 2.533 Å (300 K) to 2.490 Å (10 K) and from 3.183 Å to 3.154 Å, respectively, evidencing an increasing strength of the hydrogen bonds. The H···H distances also decrease from 2.055 Å to 2.018 Å causing enlarged interatomic repulsion (Lutz 1995). In the case of very weak hydrogen bonds, there is a complicated competition of different effects such as hydrogen bonding, proton-proton repulsion, and polarization of the intraionic O–H bonds by adjacent metal ions (Lutz 1995). This competition can be acute at high pressure and gives rise to structural frustration, seen in spectroscopic data as a dramatic broadening of the O-H stretching mode (Nguyen et al. 1994). Recent results suggest that at high pressures the effects of H…H repulsion dominate the interlayer forces in these materials (Parise et al. 1999).

Magnetic ordering

The magnetic moment obtained from a full Rietveld refinement is 3.57(2) μ_B at 10 K, somewhat less than the free-ion

TABLE 2. Selected interatomic distances (Å) of brucite-type $Fe(OH_{0.86}D_{0.14})_2$ at temperature

	Intralayer*				Interlayer*		
T (K)	Fe–O	O···O	O···O	O–H	O···O	H···H	H···O
10	2.141(1)	2.779(1)	3.259(1)	0.901(4)	3.154(1)	2.018(4)	2.490(3)
150	2.142(1)	2.777(1)	3.262(1)	0.872(5)	3.164(1)	2.046(4)	2.517(2)
300	2.143(1)	2.775(1)	3.265(1)	0.873(7)	3.183(1)	2.055(6)	2.533(7)

* Distances within (intra) or between (inter) layers (Fig. 1).

spin-only value of 4.9 μ_B. However, this is consistent with the lower than expected values observed in the other M^{2+}-hydroxides (M = Co, Ni, Mn; Christensen and Ollivier 1972; Parise and Marshall, in preparation; Szytula et al. 1971), which were attributed to quenching of the orbital moment by the crystal field (Szytula et al. 1971). The magnetic structure of $Fe(OH)_2$ differs from that of $Ni(OH)_2$ and β-$Co(OH)_2$ in that the moment lies in the basal plane, as opposed to being directed along the *c* axis (Szytula et al. 1971). The ferromagnetic sheets are then coupled antiferromagnetically between the layers (Fig. 3). The magnetic structure closely resembles that reported for $CoBr_2$ (Wilkinson et al. 1959). The interactions between Fe^{2+} ions are clearly of the exchange type, because the Fe-Fe distances, 3.26 Å within the layers and 4.58 Å between layers (Fig. 1), are greater than the sum of the ionic radii, 1.84 Å. Exchange takes place through the OH^- ions, with the parallel coupling within the layers occurring through the ions on either side of the octahedron around each Fe^{2+}. The second (antiferromagnetic) interaction is via Fe-OH-HO-Fe, and this couples the ferromagnetic sheets. This antiferromagnetic coupling has been shown to be relatively soft in other transition metal hydroxides (Szytula et al. 1971), where magnetic fields as weak as 40 kOe cause a spin flip to an exclusively ferromagnetic state.

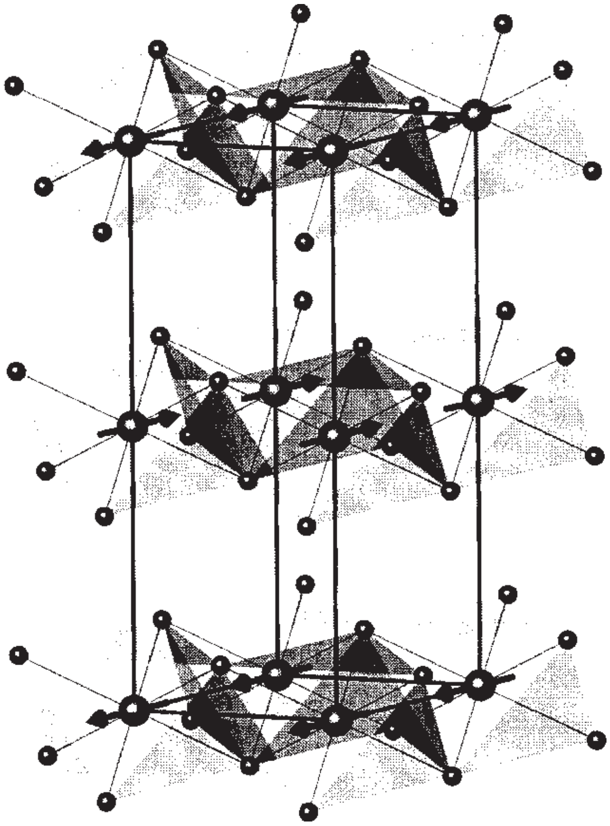

FIGURE 3. The magnetic structure of $Fe(OH_{0.86}OD_{0.14})_2$. Arrows indicate the spin directions on the Fe^{2+} atoms octahedrally coordinated with OH^- ions. One possible orientation of spins in the basal (001) plane is indicated (see text for details). Atoms (Fig. 1) were eliminated for clarity. Dark circles represent the O atoms.

The magnetic structure also differs from that of $Mn(OH)_2$, where the neutron powder diffraction data were interpreted as arising from an antiferromagnetic sequence of spins along the *c* axis, with a screw spiral propagating in the basal plane (Christensen and Ollivier 1972). The proposed magnetic structure of $Mn(OH)_2$ represents a hybrid of the antiferromagnetic coupling observed in $Fe(OH)_2$, with spins oriented exclusively in the basal plane, and that found in β-$Co(OH)_2$ and $Ni(OH)_2$, where the spins are oriented exclusively along the *c* axis. Given the relatively low quality data which may be expected for $Mn(OH)_2$ due to the high incoherent background and the small negative scattering length of Mn, a reinvestigation of the magnetic structure with a fresh sample of $Mn(OD)_2$ would be warranted. We have carried out such a study (Parise and Marshall in preparation), and full Rietveld refinement using high quality data confirms the previously reported magnetic structure.

ACKNOWLEDGEMENTS

This research was supported by the National Science Foundation through its DMR and EAR programs (MPI contribution no. 267). This work is also supported by the UK-CCLRC through access to beamtime at the ISIS facility and other support.

REFERENCES CITED

Beckenkamp, K. and Lutz, H.D. (1992) Lattice vibration spectra Part LXXII. OH stretching frequencies of solid hydroxides—correlation with structural and bonding data. Journal of Molecular Structure, 270, 393–405.

Castro, E.B. and Vilche, J.R. (1991) Electrooxidation Electroreduction Processes At Composite Iron Hydroxide Layers in Carbonate-Bicarbonate Buffers. Journal of Applied Electrochemistry, 21, 543–551.

Catti, M., Ferraris, G., and Pavese, A. (1995) Static compression and H disorder in brucite, $Mg(OH)_2$, to 11 GPa: A powder neutron diffraction study. Physics and Chemistry of Minerals, 22, 200–206.

Christensen, A.N. and Ollivier, G. (1972) Hydrothermal preparation and low temperature magnetic properties of $Mn(OH)_2$. Solid State Communications, 10, 609–614.

D'Arco, P., Causa, M., Roetti, C., and Silvi, B. (1993) Periodic Hartree-Fock study of a weakly bonded layer structure: Brucite $Mg(OH)_2$. Physical Review, B, 47, 3522–3529.

Desgranges, L., Grebille, D., Calvarin, G., Chevrier, G., Floquet, N., and Niepce, J.-C. (1993) Hydrogen thermal motion in calcium hydroxide: $Ca(OH)_2$. Acta Crystallographica, B49, 812–817.

Desgranges, L., Calvarin, G., and Chevrier, G. (1996) Interlayer interactions in $M(OH)_2$: a neutron diffraction study of $Mg(OH)_2$. Acta Crystallographica, B52, 82–86.

Duffy, T.S., Mease, C., Fei, Y., Mao, H., and Hemley, R. (1995) High Pressure phase transition in brucite, $Mg(OH)_2$. American Mineralogist, 80, 222–230.

Greaves, C. and Thomas, M.A. (1986) Refinement of the structure of deuterated nickel hydroxide, $Ni(OD)_2$ by powder neutron diffraction and evidence for structural disorder in samples with high surface area. Acta Crystallographica., B42, 51–55.

Hazen, R.M. and Finger, L.W. (1982) Comparative Crystal Chemistry. Wiley, New York.

Ivanov, V.N., Stabnikova, E.V., and Shirokikh, V.O. (1997) Effect of divalent iron oxidation on nitrification in model aquatic and soil microbial ecosystems. Microbiology, 66, 337–341.

Kruger, M.B., Williams, Q., and Jeanloz, R. (1989) Vibrational spectra of $Mg(OH)_2$ and $Ca(OH)_2$ under pressure. Journal of Chemical Physics, 91, 5910–5915.

Larson, A.C. and Von Dreele, R.B. (1986) GSAS manual. Los Alamos report LAUR 86–748.

Lutz, H.D. (1995) Hydroxide ions in condensed materials—correlation of spectroscopic and structural data, 86–103 p. Springer-Verlag, Berlin-Heidelberg.

Lutz, H.D. and Jung, C. (1997) Water molecules and hydroxide ions in condensed materials; correlation of spectroscopic and structural data. Journal of Molecular Structure, 404, 63–66.

Lutz, H.D., Möller, H., and Schmidt, M. (1994a) Lattice vibration spectra Part LXXXII Brucite type hydroxides $M(OH)_2$ (M = Ca, Mn, Co, Fe, Cd)—IR and Raman spectra, neutron diffraction of $Fe(OD)_2$. Journal of Molecular Structure, 328, 121–131.

Lutz, H.D., Beckenkamp, K., and Möller, H. (1994b) Weak hydrogen bonds in solid hydroxides and hydrates. Journal of Molecular Structure, 322, 263–266.

Lutz, H.D., Jung, C., Tromel, M., and Losel, J. (1995) Brown's bond valences, a measure of the strength of hydrogen bonds. Journal of Molecular Structure, 351, 205–209.

Megaw, H.D. (1958) Some empirical problems concerning atomic bonds. Reviews of Modern Physics, 30, 96–99.

Nguyen, J.H., Kruger, M.B., and Jeanloz, R. (1994) Compression and pressure-induced amorphization of Co(OH)$_2$ characterized by infrared vibrational spectroscopy. Physical Review B, 49, 3734–3738.

Nguyen, J.H., Kruger, M.B., and Jeanloz, R. (1997) Evidence for "partial" (sublattice) amorphization in Co(OH)$_2$. Physical Review Letters, 49, 1936–1939.

Parise, J.B., Leinenweber, K., Weidner, D.J., Tan, K., and Von Dreele, R.B. (1994) Pressure-induced hydrogen bonding: Neutron Diffraction study of brucite, Mg(OD)$_2$, to 9.3 GPa. American Mineralogist, 79, 193–96.

Parise, J.B., Cox, H., Kagi, H., Li, R., Marshall, W., Loveday, J., and Klotz, S. (1998a) Hydrogen Bonding in M(OD)$_2$ Compounds Under Pressure. Reviews of High Pressure Science and Technology, 7, 211–216.

Parise, J.B., Theroux, B., Li, R., Loveday, J., Marshall, W., and Klotz, S. (1998b) Pressure dependence of hydrogen bonding in metal deuteroxides: a neutron powder diffraction study of Mn(OD)$_2$ and β-Co(OD)$_2$. Physics and Chemistry of Minerals, 25, 130–137.

Parise, J.B., Loveday, J.S., Nelmes, R.N., and Kagi, H. (1999) Hydrogen repulsion "transition" in Co(OD)$_2$ at high pressure? Physical Review Letters, 83, 328–331.

Partin, D., O'Keefe, M., and Von Dreele, R.B. (1994) Neutron diffraction study of brucite to 10 K. Journal of Applied Crystallography, 27, 581–587.

Rietveld, H.M. (1969) A profile refinement method for nuclear and magnetic structures. Journal of Applied Crystallography, 2, 65–71.

Sherman, D.M. (1991) Hartree-Fock band structure, equation of state, and pressure-induced hydrogen bonding in brucite, Mg(OH)$_2$. American Mineralogist, 76, 1769–1772.

Smith, R.I., Hull, S., and Armstrong, A.R. (1994) The POLARIS Powder Diffractometer at ISIS Proceedings of the Third European Powder Diffraction Conference (EPDIC-3), Vienna, Austria, 1993. Materials Science Forum, 166–169, 251–256

Szytula, A., Murasik, A., and Balanda, M. (1971) Neutron diffraction study of Ni(OH)$_2$. Physica Status Solidi, 43, 125–128.

Verkhovtseva, N.V., Babanin, V.F., and Shipilin, A.M. (1991) Study of iron hydroxide transformation under the action of Azotobacter Vinelandii by means of Mossbauer-spectroscopy and magnetic measurements. Biofizika, 36, 609–613.

Wilkinson, M.K., Cable, J.W., Wollan, E.O., and Koehler, W.C. (1959) Neutron diffraction investigations of the magnetic ordering in FeBr$_2$, CoBr$_2$, FeCl$_2$ and CoCl$_2$. Physical Review, 113, 497–507.

MANUSCRIPT RECEIVED MARCH 29, 1999
MANUSCRIPT ACCEPTED SEPTEMBER 16, 1999
PAPER HANDLED BY ROBERTA OBERTI